INTERNATIONAL ATOMIC ENERGY AGENCY
UNITED NATIONS EDUCATIONAL, SCIENTIFIC AND CULTURAL ORGANIZATION
INTERNATIONAL CENTRE FOR THEORETICAL PHYSICS
34100 TRIESTE (ITALY) - P.O.B. 586 - MIRAMARE - STRADA COSTIERA 11 - TELEPHONE: 2240-1
CABLE: CENTRATOM - TELEX 460392 - I

H4.SMR/204 - 12

WINTER COLLEGE ON ATOMIC AND MOLECULAR PHYSICS

(9 March - 3 April 1987)

(ANALYTICAL LASER SPECTROSCOPY 1)

Photothermal Laser Spectroscopy

N. OMENETTO
Joint Research Centre
Ispra (Va), Italy

ICTP WINTER COLLEGE ON ATOMIC AND MOLECULAR PHYSICS

TRIESTE , March 1987

“ANALYTICAL LASER SPECTROSCOPY 1”

Lecturer : N. OMENETTO
Joint Research Centre
Ispra (Va) , Italy

IX.

☆ Photothermal Laser Spectroscopy

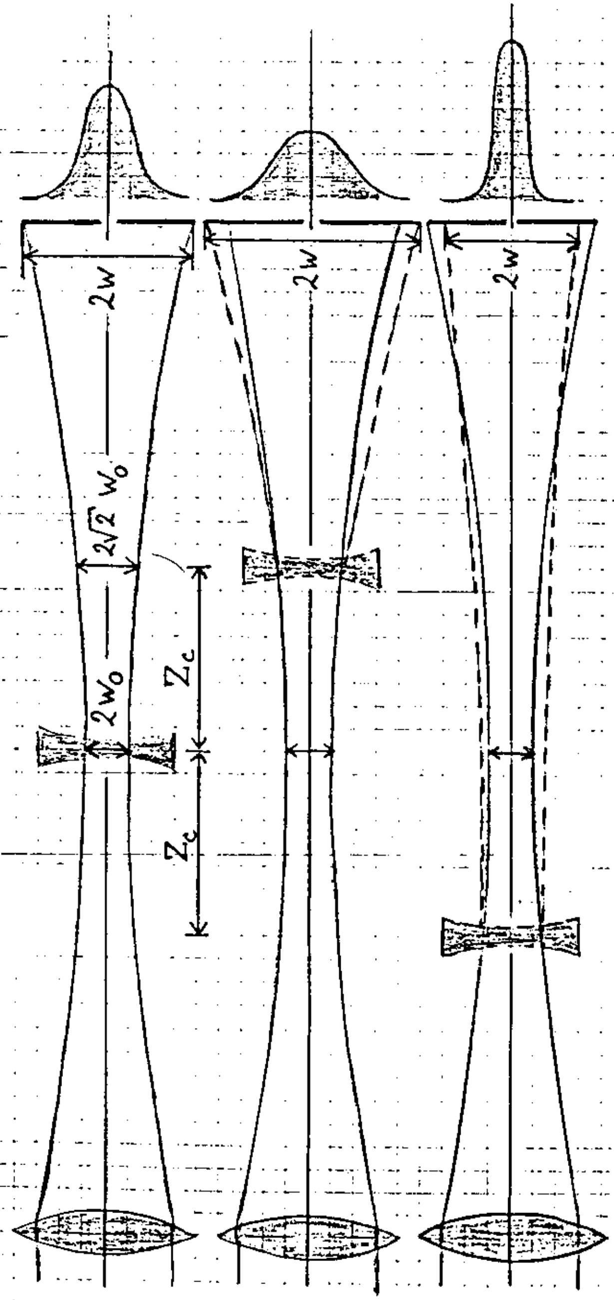

W_o = minimum waist of gaussian beam at Z = 0

$W^2 = W_o^2\left[1 + (Z/Z_c)^2\right]$

Z_c = confocal distance = $\pi W_o^2/\lambda$

I_{bc} = Intensity of the beam center sampled in the far field = $2P/\pi W^2$ where P is the total laser power.

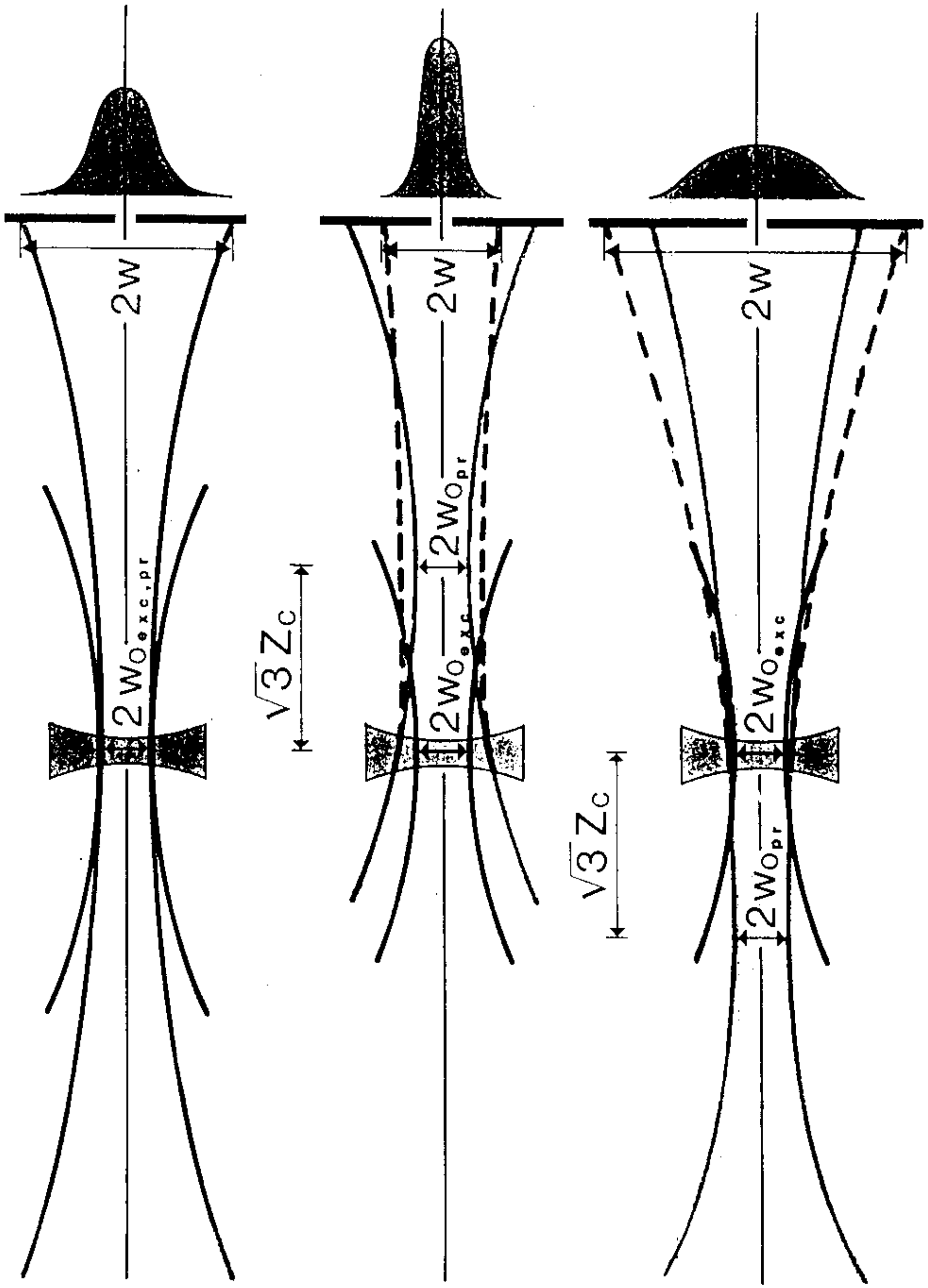

Instrumentation

Michael D. Morris
Konan Peck
Department of Chemistry
University of Michigan
Ann Arbor, Mich. 48109

Photothermal Effects in Chemical Analysis

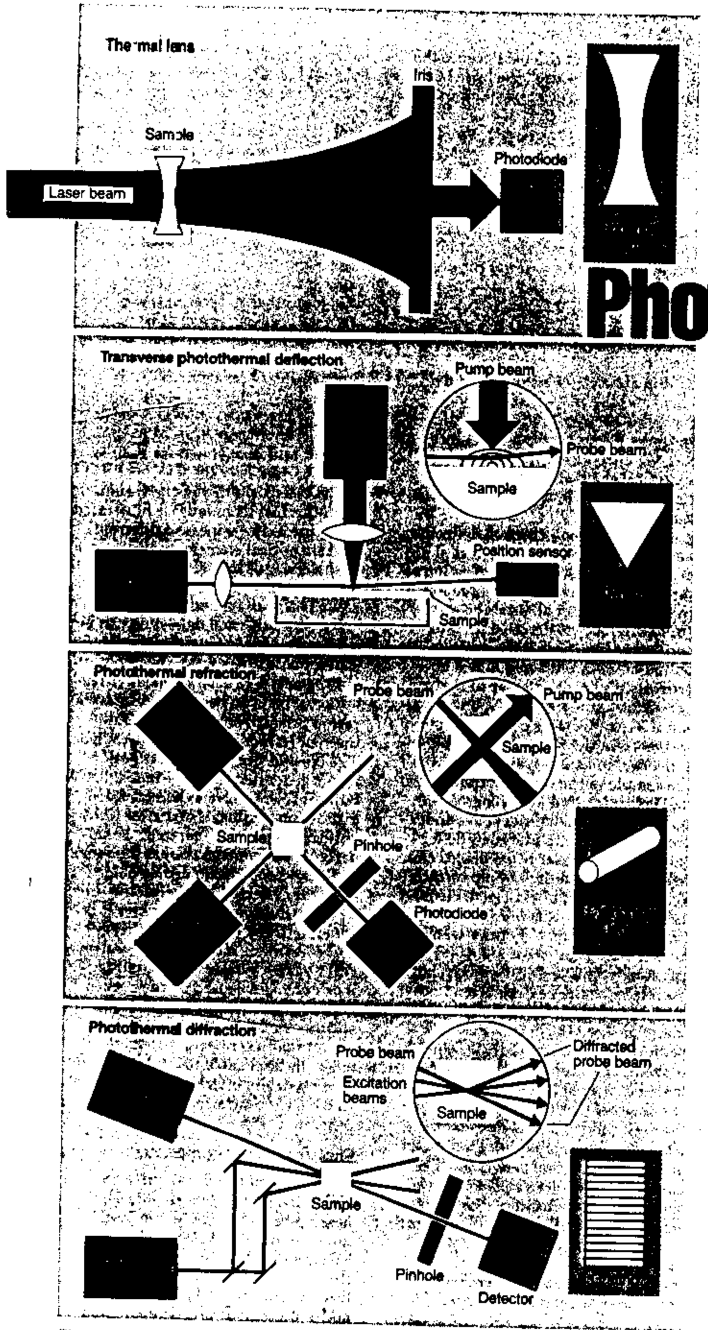

Figure 1. The principles of four widely used photothermal spectroscopic techniques
The optical configuration and the discrete optical element that approximates the refractive-index distribution are shown

In his *Travels* Marco Polo wrote, "It is said that some persons, in their course across the desert, have seen what appeared to them to be a body of armed men advancing towards them, and apprehensive of being attacked and plundered have taken to flight." (*1*). The illusions in the Gobi Desert described by Marco Polo, whether exaggerated or not, are common phenomena in deserts and other areas of high temperature throughout the world. It is now well understood that these bands of desert marauders are mirages. They are simply the effect of unsteady refractive-index distributions caused by dissipation into the air of the energy absorbed by the earth from the intense desert sunlight.

On the laboratory scale, refractive-index distributions produced by light absorption and consequent local heating are increasingly useful phenomena. These are the effects used in photothermal spectroscopies, an emerging class of ultrasensitive absorption spectroscopies. Laser light, rather than sunlight, is the usual energy source. In liquids or gases or weakly absorbing solids, the refractive-index changes are probed in the absorbing medium itself. Opaque or highly scattering solids, such as powders, are probed by the refractive-index gradient generated in a coupling fluid in contact with the solid.

Many experimental configurations have been used to probe these two

0003-2700/86/0358-811A$01.50/0

kinds of systems. The principles of four popular approaches are outlined in Figure 1. The refractive-index distribution generated by each experiment approximates a conventional optical element. That element is shown next to each configuration.

By far the most common effects used are transverse photothermal deflection, also called the mirage effect, and the thermal-lens effect. Transverse photothermal deflection probes the refractive-index change of the medium in thermal contact with the sample, whereas the thermal-lens technique probes the change of refractive index of the sample directly. The thermal lens can be observed as the defocusing of the laser that heats the solution, or as the defocusing of a second weak probe beam. Variants in which the lens is observed with a nonparaxial probe laser are increasingly common. Depending on the details of the experiments, and the laboratories reporting them, these techniques are called collinear photothermal deflection or crossed-beam thermal-lens measurements.

Photothermal effects are closely related to the photoacoustic effect. In photoacoustic measurements, the heat generated by light absorption is detected as a pressure change, using a microphone or other pressure transducer in contact with the sample or a coupling fluid. Both photoacoustic and photothermal spectroscopy are indirect absorption measurements.

To the extent that a sample is embedded in a nonabsorbing matrix, photothermal and photoacoustic spectroscopies are zero background measurement techniques. They should provide for nonfluorescent systems the same advantage that fluorimetry offers, which is the absence of shot noise associated with measurement of a large background signal. This advantage is more easily realized in gases than in liquids or solids. In principle, photoacoustic and photothermal measurements are capable of measuring absorbances down to 10^{-9} units, although this level is rarely reached. By that standard, nominally transparent materials, which may have absorbances of 10^{-6}–10^{-3}/cm, are strongly absorbing. In condensed-phase measurements photothermal techniques are often limited by the noise associated with matrix absorption.

The thermal lens effect was first observed in the early years of laser Raman experiments by Gordon and coworkers (*2*). They observed that the small amount of heat deposited in a liquid benzene sample caused local heating. The heat, in turn, formed a refractive-index distribution that behaved as a diverging lens. Because the thermal lens defocused the laser beam that generated it, even small absorbances were easily detected as changes in the spot size of the laser beam.

Thermal-lens spectroscopy was soon applied in the physics community for measurement of visible light absorption by pure organic liquids. By the early 1970s, the technique was used by Flynn and his co-workers to study vibrational energy transfer in the gas phase (*3*). In the mid-1970s Albrecht and Swofford (*4*) introduced a convenient two-laser variant for liquid phase measurements, and Kliger and Twarowski (*5, 6*) began a study of two-photon absorption using pulsed dye lasers and thermal-lens detection. Harris's INSTRUMENTATION article on thermal-lens theory in this JOURNAL (*7*) introduced the technique to analytical chemists and sparked the current interest in applications of this technique.

Transverse photothermal deflection was first reported by Boccara et al. (*8*) in 1980. The effect is an application of the mirages described by Marco Polo. In fact, Boccara et al. used the term "mirage effect" to describe their experiments. The heating beam is pulsed or modulated and aimed approximately perpendicular to the sample surface. It is frequently, but not always, a laser beam. The energy absorbed from the heating beam and converted to heat is transferred from the sample to the coupling fluid above it. The transferred heat generates a pulsed or modulated refractive-index gradient that is monitored as deflection of a probe laser beam placed close to and parallel to the sample surface. Within a year, applications to chemical spectroscopy began. Among the first was detection of Fourier transform infrared spectra of solids (*9*). Interestingly, this application does not use a laser as the heating beam.

The term photothermal deflection is sometimes used to describe several photothermal effects that cause a probe laser beam deflection, rather than a change of focus only. Detection of a thermal lens by measurement of the deflection of a probe beam placed off-center in the lens (*10*) is called collinear photothermal deflection. The mirage effect is often called transverse photothermal deflection. Photothermal displacement is the label for measurement of the photothermally induced distortion of the surface of a smooth solid sample by deflection of a probe laser beam reflected from it (*11*).

To compound the confusion, probing the thermal lens in a sample at right angles to the laser beam that caused it is called photothermal refraction (*12, 13*). As shown in Figure 1, the thermal lens will appear as a cylindrical lens to the probe beam. The photothermal-refraction configuration minimizes the probed volume in the sample and provides the best spatial resolution of the single-phase photothermal experiments.

Diffractive photothermal effects can be generated with two crossed laser beams and probed with a third. These experiments are called transient gratings, photothermal gratings, phase gratings, or holographic measurements. In principle (and sometimes in practice) they provide the best sensitivity and the best temporal and spatial resolution of all of the photothermal measurements. However, the grating experiments are also the most difficult and least suited for routine analytical use.

The essential unity of the various photothermal techniques is illustrated by Figure 1. In each case a different discrete optical element approximates the behavior of the refractive-index distribution as generated and measured. The thermal lens effect and collinear photothermal deflection can be represented by a spherical lens. The experiments differ only in whether or not the lens is probed paraxially. The mirage effect can be modeled by an inverted prism. The model for photothermal refraction is a cylindrical lens. The crossed heating-beam experiments generate refractive-index distributions that behave as transmission diffraction gratings. No matter what optical element is generated, the underlying phenomena remain the same.

A laser probe beam can be defocused or deflected by a refractive-index distribution, no matter how it is generated. For example, McCreery and co-workers have studied electrode reactions by monitoring the refractive-index changes caused by the concentration gradient near the electrode surface (*14*). Pawliszyn recently suggested that laser beam deflection might be applicable to a large number of analytically interesting systems in which a concentration distribution is generated (*15*).

Photothermal instrumentation

In a typical transverse photothermal deflection system (Figure 1), the heating beam is a low-power laser, modulated at 5–20 Hz with a mechanical chopper. The periodic deflection of the low-power helium-neon probe beam is monitored with a razor blade and a photodiode and demodulated with a lock-in amplifier. A position-sensing photodiode can replace the razor blade photodiode. A pulsed laser can be used in place of the continuous-wave (CW) laser, with gated integration in place of lock-in demodulation. Other variants on this design include use of an arc lamp and monochromator as the heating beam and use of carbon tetrachloride rather than air as the coupling fluid.

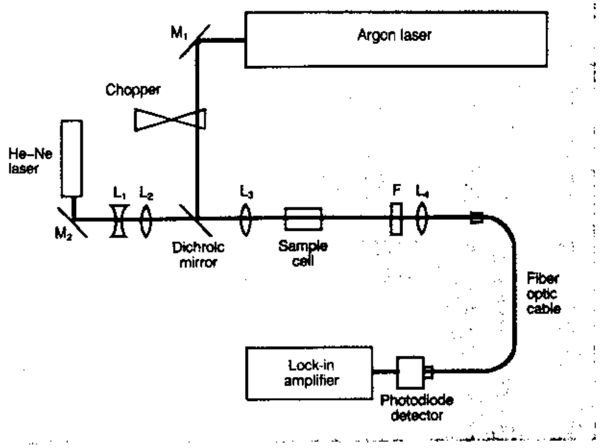

Figure 2. Pump–probe thermal lens system

The lens is generated with a modulated argon ion laser and probed with a much weaker He–Ne laser. L = lens, M = mirror, F = filter. (Reprinted from Buffett, C. E.; Morris, M. D. *Anal. Chem.* **1982**, *54*, 1824–25)

For quantitative analysis the concentrations or quantities of samples can be obtained simply by calibration at a fixed wavelength with standards. If the wavelength of the pump beam is varied, the deflection of the probe beam is then a measure of the absorption spectrum of the sample investigated. For this purpose, an incoherent heating beam is usually more convenient than a laser.

A thermal-lens measurement can be made using only a single laser because the beam that generates the lens is itself defocused. The strength of the lens can be measured by estimating the steady-state defocusing as the reduced transmission through a small aperture located some distance beyond the sample. Harris and co-workers have demonstrated that measurement of the complete time evolution of the thermal lens provides superior results (*16*). They measure the intensity decrease over a period of 0.01–1.0 s. The data are fitted to the thermal-lens equation (see below) to derive the sample absorbance.

Some groups use independent heating (pump) and probe laser beams, as introduced by Albrecht and Swofford (*4*). With a modulated CW laser, the two-beam system can use convenient lock-in amplifier signal processing of the probe beam defocusing signal. Careful comparison has shown that one- and two-beam systems provide essentially identical detection limits (*17*). A two-beam system is required with pulsed lasers because the laser pulse duration is much shorter than the response time of the thermal lens itself. Two-beam systems are also required for nonparaxial probes of the thermal lens, as in collinear photothermal deflection or photothermal refraction.

Figure 2 shows a typical two-beam thermal-lens measurement system. The heating laser is an argon ion laser, usually operated with 20–100-mW output. The beam is modulated with a mechanical chopper and combined collinearly with a helium–neon probe beam. The combined beams are focused into the sample with a short (30–100 mm, depending on the application) focal-length lens. A simple glass filter is used to isolate the probe beam beyond the sample. An optical fiber serves as the limiting aperture and also to relay the probe beam to a photodiode. Similar systems, with different probe beam orientations, are used for photothermal refraction and collinear photothermal deflection.

Low-power (0.5–2-mW) He–Ne lasers are the most commonly used probes for photothermal measurements. Modern designs provide stable outputs and nearly ideal Gaussian beams. The lasers are inexpensive and have operating lifetimes of 10,000-20,000 h.

Theory

A rigorous treatment of most photothermal effects leads to intractable equations. Simplifying assumptions are necessary. Typically, these work well for small refractive index distributions, as encountered at low absorptions or with low laser powers; however, they may not be quantitatively correct if the photothermal effect is strong.

Gordon and co-workers presented the first theoretical treatment of thermal-lens theory. Their treatment was used by Hu and Whinnery (*18*) to describe the one-laser thermal lens measurement system. We use the modifications of Carter and Harris (*19*), which successfully account for lens aberrations (*20*).

If the illuminating laser is turned on at some time $t = 0$, the intensity, $I(t)$, through the limiting aperture is given by Equation 1.

$$\frac{I(t)}{I(0)} = \frac{1}{\left[1 - \dfrac{\theta}{1 + \dfrac{t_c}{t}} + \dfrac{\theta^2}{2\left(1 + \dfrac{t_c}{t}\right)^2}\right]} \tag{1}$$

The sample absorbance is included in θ, defined by Equation 2.

$$\theta \equiv \frac{1.19PA\left(\dfrac{dn}{dT}\right)}{\lambda k} \tag{2}$$

P is the absorbed laser power, which is proportional to the incident power (P_0) and the absorbance (A), k is the thermal conductivity, and λ is the wavelength. The critical time (t_c) is $t_c \equiv w_1^2/4D$ where w_1 is the beam radius at the sample and D, the thermal diffusivity of the sample.

Equation 1 is an adequate description of the thermal-lens effect obtained with CW lasers, at least up to absorbance 0.01. Related equations are obtained for the two-laser systems using pulsed lasers or modulated CW lasers. In all cases the equations predict that the response will contain terms that are linear and quadratic in concentration and time. This fundamental nonlinearity is a minor complication for absorbance measurements above about 0.001. For weakly absorbing samples, a linear concentration response is usually observed.

The quantity in Equation 3,

$$\theta/A = 1.19\,P(dn/dT)/\lambda k \tag{3}$$

is often called E, the enhancement factor, in the analytical literature (*7*). The enhancement factor is the relative thermal-lens response. Enhancement factors for common solvents have been tabulated by Harris and Dovichi. They range from about 0.14 for water, through 1.7 for methanol, to 4.7 for carbon tetrachloride, for 1-mW laser power. In all photothermal spectroscopies, the ratio of refractive-index coef-

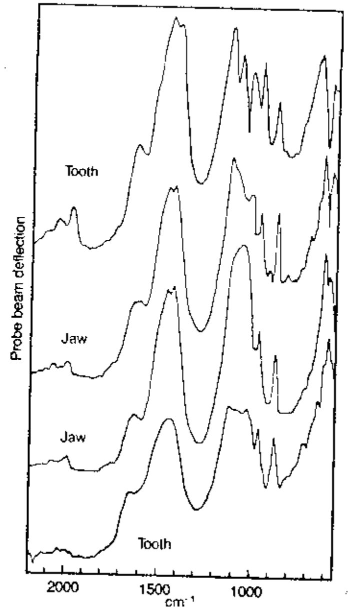

Figure 3. IR photothermal deflection spectra of Mesohippus jaw bone and tooth, Oligocene, White River formation, South Dakota

Spectra are from different positions on the fossil. (Reprinted with permission from Reference 23)

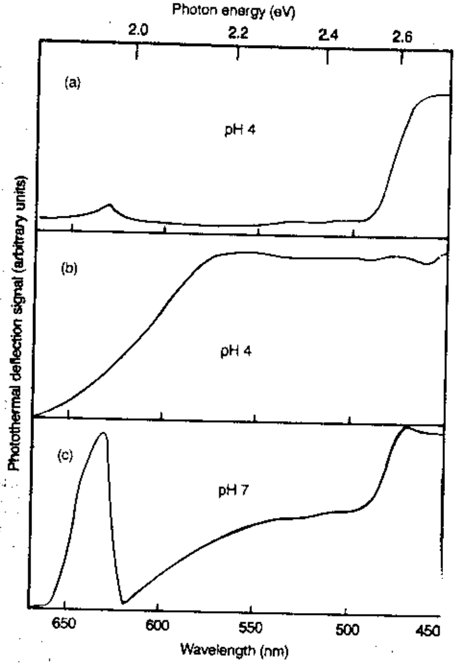

Figure 4. Photothermal deflection spectra of ZnSe photocorrosion

(a) pH 4, 20 min at 460 nm. (b) pH 4, 18 h at 460 nm. (c) pH 7, 18 h at 460 nm. (Reprinted with permission from Reference 31)

ficient to thermal conductivity will govern the sensitivity. It is clear that water is not the best choice of solvent for thermal-lens experiments. Compared with other solvents water has a small refractive-index temperature coefficient, which contributes to a weak thermal lens. It also has a large thermal conductivity, which contributes to rapid dissipation of the lens.

Equation 4 is the basic transverse photothermal deflection response for a sinusoidally modulated heating beam.

$$\phi = \frac{dn}{dT}\,\frac{2\alpha PL}{\rho C(\omega D_g)^{1/2}} \qquad (4)$$

It is valid in the limit of low absorbance. A related equation describes the response to a pulsed heating beam.

In Equation 4, ϕ is the deflection angle, α is the absorption per unit length of sample, L is the length of sample illuminated, ρ is the density of the sample, C is its specific heat, ω is the (angular) modulation frequency, and D_g is the thermal diffusivity of the coupling fluid over the sample. The heating beam is assumed to have a uniform power density across the illuminated region. The probe laser beam is assumed to have a uniform cross section. Equation 4 assumes that the refractive index is perturbed in the vertical direction only. This assumption can be relaxed (*21*).

Some limitations

Several factors determine the signal-to-noise (S/N) ratio in photothermal measurements. In general, the intensities of photothermal effects increase linearly with power density. A tightly focused pump beam gives a better S/N ratio than a loosely focused beam. At constant beam cross-section area, increased pump beam power can be used to increase the signal. In either case, the signal becomes saturated beyond certain power densities.

More commonly, above some threshold, noise sources increase proportionally with signal. Proportional noise sources include unstable intensity and beam pointing jitter in the heating and probe laser beams, mechanical vibration of apparatus, and motion of the material in which the refractive index is created. Examples include random air currents perturbing photothermal deflection and flow fluctuations breaking up thermal lenses formed in chromatographic effluents. These effects can reduce S/N ratios by at least an order of magnitude. Detector electronics noise can usually be reduced to insignificant levels by proper choice of components and signal processing techniques

In the refractive-index distribution generated in any photothermal technique, there is a sample region with maximum refractive-index change. Probing this region yields maximum sensitivity. In each of the two laser techniques, careful alignment is required to achieve optimum S/N ratio or even reproducible results. In a single-beam thermal-lens experiment, judicious choice of placement and size of the limiting aperture is necessary.

In many analytical applications photochemical reactions are potentially a serious source of error in transverse photothermal deflection measurements or any other measurements of solids. In a liquid or gaseous sample, diffusion and convection provide at least partial replenishment of the sample. In a solid, the same population of molecules is irradiated as long as the laser is incident on the same region. Samples can be visibly decomposed with tightly focused pulsed lasers, and, in some cases with tightly focused CW lasers as well. Cis-trans photoisomerization can cause systematic errors in photothermal examination of compounds containing C=C, C=N, or N=N bonds, even if the incident laser power is only a few milliwatts (*22*).

Analytical applications

Photothermal effects are useful in characterizing physical and chemical properties of a wide variety of solid, liquid, and gaseous materials. In this review, we describe only condensed-phase applications, with emphasis on those of current or potential use to analytical chemists.

Materials studies. Low and coworkers have investigated photothermal deflection as an alternative to photoacoustic spectroscopy for detection of infrared (IR) spectra of solids. They have modified a conventional Fourier transform spectrometer to accommodate a probe laser and position sensor. They have demonstrated the utility of this system for examination of large, irregular samples that cannot be accommodated in a closed photoacoustic cell. Their work also shows the superior sensitivity of photothermal deflection detection in this application. The trade-off is a somewhat increased complexity, as the probe laser beam must be positioned carefully over the sample if quantitative measurements are desired. The photothermal technique has been applied to the study of samples as diverse as fossils (*23*), minerals (*24*), and human hair (*25*). The spectra of fossilized Mesohippus jawbone and tooth samples are shown in Figure 3.

Photothermal deflection using a xenon arc lamp has been used to obtain the absorption spectrum of powdered minerals, including those used as photoelectrochemical surfaces (*26*). Both interferometers and dispersive monochromators have been used to obtain UV–vis spectra of materials (*27*).

Photoacoustic spectroscopy has been applied to the in situ study of metal–electrolyte interfaces (*28*). Photothermal deflection is three orders of magnitude more sensitive than photoacoustic measurements of absorbing species at a solid–liquid interface (*29*). The photothermal deflection technique has been used to monitor the electrochemical deposition of a thin layer of metal or oxide on a metallic electrode (*30*) and to study the photocorrosion of semiconductors (*31*). Figure 4 shows photothermal deflection spectra of the thin films of selenium generated by a blue light illumination of ZnSe immersed in electrolytes.

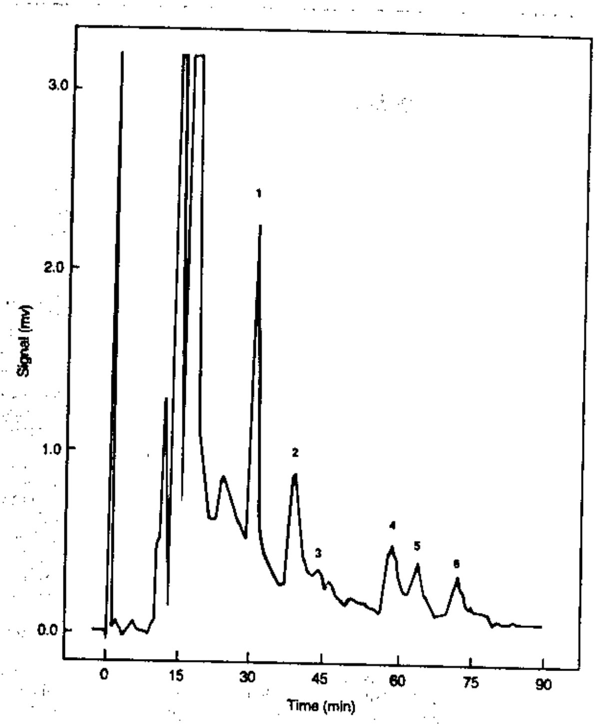

Figure 5. High-performance liquid chromatography chromatogram of 120 fmol of each of six amino acids

Peak 1, glycine; 2, proline; 3, methionine; 4, tryptophan; 5, leucine; and 6, phenylalanine. (Reprinted from Reference 36 with permission of the Electrochemical Society Inc.)

Photothermal effects can also be used to measure the thermal properties of materials. For example, the rate of dissipation of the thermal lens is a quantitative measurement of thermal diffusivity. The major thermal-lens measurement schemes have been used in this application (*32*).

Chromatography. Several groups are engaged in development of photothermal spectroscopies as detectors for liquid chromatography (LC). Applications to microbore (*33, 34*) and capillary (*35*) column chromatography appear to be most promising. The detector volume constraints of microbore and capillary columns are no impediment. Strong thermal-lens signals are easily generated in volumes of a few nanoliters or even picoliters. For example, Figure 5 shows the detection of 120-fmol quantities of several amino acids separated on a microbore column. The experiment uses the photothermal refraction configuration with a working volume of a few picoliters.

Thermal-lens LC detectors have recently achieved noise levels of 0.1 microabsorbance (*34, 36*). The extraordinary sensitivity results from the combination of good optical design with the use of a low pulsation pump to eliminate flow fluctuation noise. By contrast, the latest conventional commercial absorbance detectors have noise levels of about 10–20 microabsorbance. Earlier thermal lens detectors reached 1-microabsorbance noise levels but were unable to penetrate that barrier.

Much of the exploratory work has been carried out with argon ion laser sources, operating in the mid-visible region. It is clear that widespread utility will require operation in the UV region, especially 200–300 nm. However, the current high cost and complexity of UV lasers have restricted their use to a few specialists.

Although most attention has been focused on LC, supercritical fluid chromatography (*37*) is another promising area. The enhancement factor for supercritical carbon dioxide is about 150 times greater than that of carbon

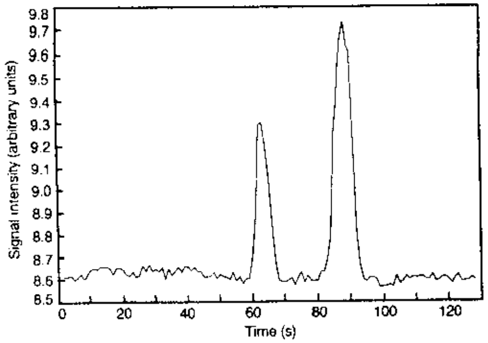

Figure 6. Scanned photothermal deflection signals from 2,4-dinitroaniline on high-performance thin-layer chromatography plates, 15- and 25-ng samples

The mirage is created by a pulsed laser (XeF, 2 mJ/pulse)

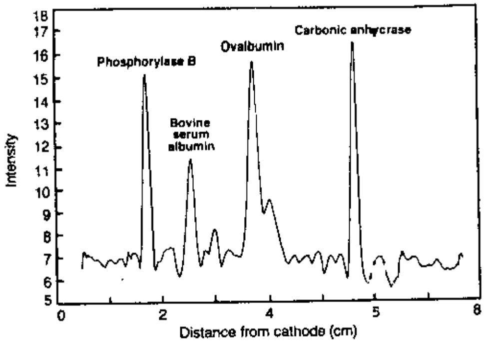

Figure 7. Thermal-lens signals from 30 ng each of four proteins separated on polyacrylamide gel

The stain is Coomassie Brilliant Blue R250

tetrachloride. Detection limits of 0.2 microabsorbance are reached in flow systems.

Transverse photothermal deflection with CW laser sources has been used for quantitation of samples on silica thin-layer chromatographic plates (22, 38). Only low (20–30 mW) heating laser power is required to reach detection limits somewhat lower than are obtainable by diffuse reflectance (22). Figure 6 shows an example of photothermal deflection using a pulsed excimer laser as the source.

Ironically, in chromatographic applications the excellent spatial resolution of photothermal deflection may be a disadvantage. Laser beams are easily shaped to allow probing of a spot of 10–50-μm diameter. However, thin-layer chromatographic spots and many other samples are rarely sufficiently uniform to warrant this kind of spatial resolution. Tightly focused laser beams probe local fluctuations in sample concentration. A fluctuating sample distribution may arise from irregularities in the plate coating or nonuniform distribution of chromogenic reagent, for example. Unless the irregularities themselves are of interest, some spatial averaging is usually desirable.

Miscellaneous. The thermal-lens detection method has been explored for other analytical applications. Thermal-lens measurements of phosphomolybdate blue have been proposed for ultratrace phosphorus analyses in natural waters (*39, 40*). In this application, dye lasers and inexpensive semiconductor diode lasers are satisfactory. Leach and Harris (*41*) have used thermal-lens spectroscopy for monitoring flow injection analyses. Thermal-lens spectroscopy has been used to quantify proteins separated by polyacrylamide gel electrophoresis (*42, 43*). The technique has proven to be about two orders of magnitude more sensitive than conventional densitometry of gels and can use small helium–neon or argon ion lasers to generate the thermal lens. A typical example is shown in Figure 7.

Thermal-lens techniques need not be limited to liquid- or gas-phase samples. Burgi and co-workers have used photothermal refraction to probe localized absorption of transition metal impurities in sphalerite, a zinc sulfide mineral (*44*). They reported a spatial resolution of about 10^{-8} cm^3.

Continuing progress in laser technology is expanding the range of compact and inexpensive lasers that are well suited for photothermal measurements. The first reports of the use of semiconductor lasers for photoacoustic and thermal-lens measurements have already appeared (*40, 45*). Wider availability of these and other small, affordable lasers should bring a rapid increase in the number of problems readily solved by photothermal spectroscopy.

References

(1) Polo, Marco. *The Travels of Marco Polo*; Doubleday & Company: New York, 1948.
(2) Gordon, J. P.; Leite, R. C. C.; Moore, R. S.; Porto, S. P. S.; Whinnery, J. R. *J. Appl. Phys.* **1965**, *36*, 3–8.
(3) Grabiner, F. R.; Flynn, G. W.; Siebert, D. R. *Chem. Phys. Lett.* **1972**, *17*, 189–94.
(4) Swofford, R. L.; Long, M. E.; Albrecht, A. C. *J. Chem. Phys.* **1976**, *65*, 179–90.
(5) Twarowski, A. J.; Kliger, D. S. *Chem. Phys.* **1977**, *20*, 253–58.
(6) Twarowski, A. J.; Kliger, D. S. *Chem. Phys.* **1977**, *20*, 259–64.
(7) Harris, J. M.; Dovichi, N. J. *Anal. Chem.* **1980**, *52*, 695–706 A.
(8) Boccara, A. C.; Fournier, D.; Badoz, J. *Appl. Phys. Lett.* **1980**, *36*, 130–32.
(9) Low, M.J.D.; Lacroix, M.; Morterra, C. *Appl. Spectrosc.* **1982**, *36*, 1552–84.
(10) Jackson, W. B.; Amer, N. M.; Boccara, A. C.; Fournier, D. *Appl. Opt* **1981**, *20*, 1333–44.
(11) Olmstead, M. A.; Amer, N. M.; Kohn, S.; Fournier, D.; Boccara, A. C. *Appl. Opt.* **1982**, *32*, 141–54.
(12) Dovichi, N. J.; Nolan, T. G.; Weimer, W. A. *Anal. Chem.* **1984**, *56*, 1700–1704.
(13) Norlan, T. G.; Weimer, W. A.; Dovichi, N. J. *Anal. Chem.* **1984**, *56*, 1704–7.
(14) Jan, C.-C.; Lavine, B. K.; McCreery, R. L. *Anal. Chem.* **1985**, *57*, 752–58.
(15) Pawliszyn, J.; Weber, M. F.; Dignam, M. J.; Mandelis, A.; Venter, R. D.; Park, S.-M. *Anal. Chem.* **1986**, *58*, 236–42.
(16) Dovichi, N. J.; Harris, J. M. *Anal. Chem.* **1981**, *53*, 106–9.
(17) Carter, C. A.; Harris, J. M *Anal. Chem.* **1983**, *55*, 1256–61.
(18) Hu, C.; Whinnery, J. R. *Appl. Opt.* **1973**, *12*, 72–79.
(19) Carter, C. A.; Harris, J. M. *Appl. Opt.* **1984**, *23*, 476–81.
(20) Sheldon, S. L.; Knight, L. V.; Thorne, J. M. *Appl. Opt.* **1982**, *21*, 1663–68.
(21) Aamodt, L. C.; Murphy, J. C. *J. Appl. Phys.* **1983**, *54*, 581–91.
(22) Peck, K.; Fotiou, F. K.; Morris, M. D. *Anal. Chem.* **1985**, *57*, 1359–62.
(23) Low, M.J.D.; Morterra, C *Appl. Spectrosc.* **1984**, *38*, 807–12.
(24) Low, M.J.D.; Tascon, J.M D. *Phys. Chem. Miner.* **1985**, *12*, 19–22.
(25) Low, M.J.D.; Severdia, A. G. *Spectrosc. Lett.* **1983**, *16*, 871–77.
(26) Tamor, M. A.; Hetrick, R E. *Appl. Phys. Lett.* **1985**, *46*, 460–62
(27) Weinberger, B. R.; Roxlo, C. B.; Etemad, S.; Baker, G. L.; Orenstein, J. *Phys. Rev. Lett.* **1984**, *53*, 86–89.
(28) Sander, U.; Strehlow, H. H.; Dohrmann, J. K. *J. Phys. Chem.* **1981**, *85*, 447–50.
(29) Fournier, D.; Boccara, A. C.; Badoz, J. *Appl. Opt.* **1982**, *21*, 74–76.
(30) Roger, J. P.; Fournier, D. Boccara, A. C. *J. Phys. Colloq.* **1983**, *44*, C6-313–C6-316.
(31) Royce, B.S.H.; Sánchez-Sinencio, F.; Goldstein, R.; Muratore, R.; Williams, R.; Yim, W. M. *J. Electrochem. Soc.* **1982**, *129*, 2393–95.
(32) Gupta, M. C.; Hong, S.-T.; Gupta, A.; Moacanin, J. *Appl. Phys. Lett.* **1980**, *37*, 505–7.
(33) Buffett, C. E.; Morris, M D. *Anal. Chem.* **1983**, *55*, 376–78.
(34) Collette, T. W.; Parekh, N. J.; Griffin, J. H.; Carreira, L. A.; Rogers, L. B. *Appl. Spectrosc.*, **1986**, *40*, 164–69.
(35) Sepaniak, M. J.; Vargo, J. D.; Kettler, C. N.; Muskarinec, M. P. *Anal. Chem.* **1984**, *56*, 1252–57.
(36) Nolan, T. G.; Hart, B. K.; Dovichi, N. J. *Anal. Chem.* **1985**, *57*, 2703–5.
(37) Leach, R. A.; Harris, J. M. *Anal. Chem.* **1984**, *56*, 2801–5.
(38) Masujima, T.; Sharda, A. N.; Lloyd, L. B.; Harris, J. M.; Eyring, F. M. *Anal. Chem.* **1984**, *56*, 2977–79.
(39) Fujiwara, K.; Lei, W.; Uchiki, H.; Shimokoshi, F.; Fuwa, K.; Kobayashi, T. *Anal. Chem.* **1982**, *54*, 2026–29.
(40) Nakanishi, K.; Imasaka, T.; Ishibashi, N. *Anal. Chem.* **1985**, *57*, 1219–23.
(41) Leach, R. A.; Harris, J. M. *Anal. Chim. Acta* **1984**, *164*, 91–101.
(42) Peck, K.; Morris, M. D. *Anal. Chem.* **1986**, *58*, 507–9.
(43) Peck, K.; Morris, M. D. submitted for publication.
(44) Burgi, D. S.; Nolan, T. G.; Risfelt, J. A.; Dovichi, N. J. *Opt. Eng.* **1984**, *23*, 756–58.
(45) Kawabata, Y.; Kamikubo, T.; Imasaka, T.; Ishibashi, N. *Anal. Chem.* **1983**, *55*, 1419–20.

Analytica Chimica Acta, 153 (1983) 265—269
Elsevier Science Publishers B.V., Amsterdam — Printed in The Netherlands

Short Communication

DETERMINATION OF LOW LEVELS OF URANIUM(VI) IN WATER SOLUTIONS BY MEANS OF THE LASER-INDUCED THERMAL LENSING EFFECT

T. BERTHOUD and P. MAUCHIEN
CEA, Centre d'Etudes Nucleaires, Fontenay aux-Roses (France)
N. OMENETTO* and G. ROSSI
Joint Research Centre, Chemistry Division, Commission of the European Communities, Ispra-Varese (Italy)

(Received 16th March 1983)

Summary. Thermal lensing spectrometry based on a pulsed, excimer-pumped, tunable dye laser as heating beam and a He—Ne laser as probe is described for the determination of low concentrations of uranyl ions in water solution. The dye laser, tuned at 414 nm, has a peak power of about 200 kW and a bandwidth of 0.02 nm. The smallest detectable sorptivity was 3×10^{-5} cm^{-1} and the limit of detection for uranium was 4×10^{-6} M.

Knowledge of the migration mechanisms of actinide ions in ground waters is necessary for safety assessments of nuclear waste deposits in rock formations. Classical analytical techniques are usually too insensitive to detect very low concentrations of these elements. For example, counting techniques are unsuitable for plutonium and neptunium, because of their very long lifetimes. Determination of the oxidation state of these elements is also of major interest for the understanding of their physico-chemical behavior at trace levels. New techniques that could detect and possibly identify the oxidation state of specific actinide ions in solutions are therefore being sought.

Thermal lensing spectroscopy, based on laser excitation, seems to be a very promising approach for actinide determinations [1]. This technique, first described by Gordon et al. [2], has been developed extensively in recent years [3—11]. As in classical absorption spectrophotometry, incident radiation is absorbed by the species to be determined; if the resulting fluorescence is weak, the absorbed energy is converted to heat which is then dissipated into the medium. When a laser is used for excitation, the beam can be focused into the absorbing medium, creating a strong local temperature gradient and so a refractive index gradient. Gordon et al. [2] showed that in the case of a gaussian laser beam (TEM_{00}), spatial redistribution of the refractive index makes the absorbing medium behave as a thin optical lens. Absorption of the incident beam can then be detected by monitoring the focusing or defocusing of the light beam passing through the absorbing medium. This is usually done by sensing the relative variation of the intensity of the laser beam passing through a small pinhole at some distance from the absorbing medium. The intensity change can be observed on the beam causing the absorption or on a probe beam, collinear with the primary beam but not absorbed by the medium. In the latter case, the creation of the thermal lens may be observed by deflection of the probe beam [12, 13] or by its defocusing. Thorough theoretical descriptions are available [2, 3, 5, 7].

Different experimental arrangements have been based on continuous wave lasers (argon ion) or pulsed dye lasers. These earlier studies have demonstrated that the technique can detect absorptions 2—3 orders of magnitude lower than is possible by conventional spectrophotometry. Further, it has been shown that water is the worst medium for development of the thermal lens effect, because of its high heat conductivity and the small temperature dependence of its refractive index compared to organic solvents such as chloroform or carbon tetrachloride. In the present case, however, water solutions were obligatory because the primary goal was to investigate the direct applicability of the technique to ground waters, without dilution or chemical treatment of the samples.

This communication presents some preliminary results obtained with pulsed dye laser excitation on uranium in pure water solutions. The choice of uranium is based on the similarity of its behavior with that of the other actinides and the fact that it does not require measures for radioprotection. Of course, the thermal lens technique cannot compete with laser-induced fluorescence of uranium in terms of sensitivity, but the results obtained with uranium indicate what can be expected for similar non-fluorescent species.

Experimental

The complete experimental set-up is schematically depicted in Fig. 1. The heating laser beam was a pulsed tunable dye laser pumped by an excimer laser. The dye laser [14] (Jobin Yvon, Longjumeau, France) consists of an oscillator cavity and one amplifier section; the excimer laser (Lambda Physik, Göttingen, Germany) was operated at the XeCl emission (308 nm). A solution of stilbene provided the necessary output in the 420-nm region and the grating was tuned to select the excitation wavelength of 414 nm with a spectral bandwidth of approximately 0.02 nm. The duration of the excitation pulse, measured with a vacuum photodiode (Model F-4000; ITT, Fort Wayne, IN, U.S.A.) and a fast oscilloscope (Tektronix Model 7904) was found to be about 6 ns. A peak power of 200 kW (≈1 mJ per pulse) was measured with a volume absorbing calorimeter (Model 380101; Scientech, Boulder, CO, U.S.A.). The dye laser beam, after spatial filtering, was focused into a quartz cell containing the uranyl solution. The thermal effect was measured by means of a He—Ne laser (Spectra Physics, Model 47430), the divergence of which was compensated by a lens. The excitation and probe beams were made collinear before crossing the sample cell by means of a

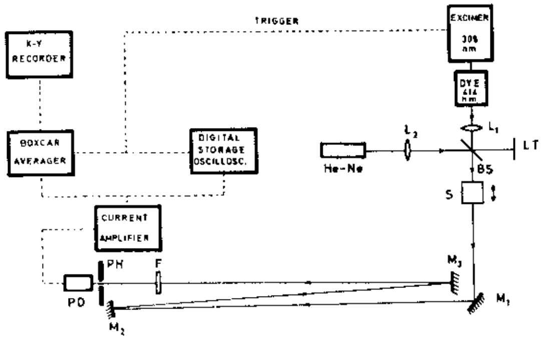

Fig. 1. Schematic layout of the system: L_1, L_2, quartz lenses; BS, beam splitter; LT, light trap; S, sample cuvette; M_1, M_2, M_3, plane mirrors; F, filter; PH, pin-hole; PD, photodiode.

quartz beam splitter. After passing through the absorbing solution, the 414-nm radiation was filtered out and the He—Ne beam was directed throughout a pinhole to a photodiode after an optical path of about 4 m. The current from the photodiode was amplified with a current amplifier (Keithley Model 427) and then sent either to a digital storage oscilloscope with averaging facilities (Tektronix Model 468) or to a boxcar integrator (Princeton Applied Research Model 162/165) connected to an X-Y recorder (Hewlett-Packard Model 7045-B). This set-up allowed retrieval of the temporal behavior of the signal and recording of the absorption spectrum by rotating the grating in the laser oscillator cavity.

Results and discussion

In order to investigate the physical characteristics of the effect caused on the probe beam by the absorbing uranyl solution when the dye laser was tuned at 414 nm, the concentration of uranium was kept at 10^{-2} M in 0.01 M nitric medium. By careful adjustment of the beam splitter, the heating and probing laser beams could be directed collinearly and/or slightly displaced throughout the absorbing volume. For 10^{-2} M uranyl nitrate, the thermal effect appeared to be a combination of both defocusing and deflection processes. This was substantiated by the clearly seen behavior of the He—Ne spot on a white screen at the position of the pinhole, and by the critical dependence of the signal observed on the pinhole position. When the concentration of the absorbing solution was decreased, no deflection effect could be seen. Beam collinearity was therefore optimized to maximize the varization of the signal which was then attributed solely to the defocusing effect, the more so because the best results were obtained when the He—Ne spot was centered on the pinhole.

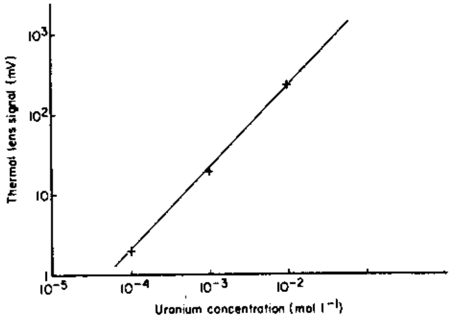

Fig. 2. Calibration graph for uranium. The thermal lensing signals were obtained with a 1-cm absorption path.

In order to assess the sensitivity of the above technique, several less concentrated solutions were tested for the thermal effect. With the 1-cm path length cell, a linear calibration curve (see Fig. 2) was easily obtained down to 10^{-4} M. With a 3-cm cell, the signal-to-noise ratio was 7 for a concentration of 10^{-5} M, averaging 256 laser pulses. This corresponds to an absorptivity of 7×10^{-5} cm^{-1}, assuming a value of 7 for the molar absorptivity of uranium at 414 nm [15]. If the detection limit is set at a signal-to-rms noise ratio equal to 3, then the minimum detectable absorptivity (3×10^{-5} cm^{-1}) corresponds to 4×10^{-6} M uranium. Needless to say, it is the product of the molar absorptivity and the molar concentration (i.e., the absorption coefficient) that matters here: considering that an aqueous medium was used, it can be seen that these measurements are within an order of magnitude of the best results previously reported [1] and obtained with more dedicated electronic data processing.

The main limitations of the present equipment are the poor stability of the He—Ne probe laser (±2%) and the limited number of pulses averaged to reduce the random noise associated with the signal. Both parameters, if properly optimized, should improve sensitivity considerably. In addition, the pulsed laser beam was not optimized in terms of its spatial structure; this could be done, for example, by inserting a small aperture in the oscillator cavity [10]. Nevertheless, the results obtained without sample treatment demonstrate that the technique is viable for the detection of actinides, and certainly worthy of further investigation.

The authors thank Dr. G. Baudin, whose interest made this work possible. The experimental help of P. Cavalli and useful discussions with Dr. H. Human are gratefully acknowledged. The work was done at the Joint Research Centre at Ispra, and was partly supported by the C.E.E. under contract WAS 210-481-7-Ss.

REFERENCES

1 J. V. Beitz and J. P. Hessler, Nucl. Technol., 51 (1980) 169.
2 J. P. Gordon, R. C. C. Leite, R. S. Moore, S. P. Porto and J. R. Whinnery, J. Appl. Phys., 36 (1965) 3.
3 C. Hu and J. R. Whinnery, Appl. Opt., 12 (1973) 72.
4 N. J. Dovichi and J. M. Harris, Anal. Chem., 52 (1980) 2338; Anal. Chem., 53 (1981) 106.
5 J. M. Harris and N. J. Dovichi, Anal. Chem., 52 (1980) 695A.
6 K. Fujiwara, H. Uchiki, F. Shimokoshi, K. Tsunoda, K. Fuwa and T. Kobayashi, Appl. Spectrosc., 36 (1982) 157.
7 S. J. Sheldon, L. V. Knight and J. M. Thorne, Appl. Opt., 21 (1982) 1663.
8 T. Imasaka, K. Miyaishi and N. Ishibashi, Anal. Chim. Acta, 115 (1980) 407.
9 K. Miyaishi, T. Imasaka and N. Ishibashi, Anal. Chim. Acta, 124 (1981) 381.
10 K. Mori, T. Imasaka and N. Ishibashi, Anal. Chem., 54 (1982) 2034.
11 K. Fujiwara, W. Lei, H. Uchiki, F. Shimokoshi, K. Fuwa and T. Kobayashi, Anal. Chem., 54 (1982) 2026.
12 D. Fournier, A. C. Boccara, N. M. Amer and R. Gerlach, Appl. Phys. Lett., 37 (1980) 519.
13 A. Rose, J. D. Pyrum, C. Muzny, G. J. Salamo and R. Gupta, Appl. Opt., 21 (1982) 2663.
14 F. Bos, Appl. Opt., 20 (1981) 3553.
15 E. Rabinowitch and R. L. Belford, Spectroscopy and Photochemistry of Uranyl Compounds, Macmillan, New York, 1964.